การประชุมวิชาการเครือข่ายวิศวกรรมเครื่องกลแห่งประเทศไทยครั้งที่ 19
19-21 ตุลาคม 2548 จังหวัดภูเก็ต

Reverse Engineering for Developing Small Hydro Turbine Using CFD Simulation

Yodchai Tiaple
Naval architecture and Marine Engineering, Faculty of Engineering Si-racha, Kasetsart University, 20230
Artit Ridluan
Research and Development Center, Summit Auto Seat Industry Ltd, Samutprakan, 10540
Noppong Sritrakul Udomkiat Nontakeaw
Department of Mechanical Engineering, King Mongkut's Institue of Technology North Bangkok, 10800
Pramote Chamamahattana
Hydro power construction division, EGAT Public company Limited, 11130

e-mail: yodchai_tp@yahoo.com, aridluan@yahoo.com, n_pp_ng@yahoo.com, unk@kmitnb.ac.th, pramote.c@egat.co.th

Abstract

Since there are thousands of potential fresh-water resources, available in THAILAND, therefore, the utilization of those fresh-water resources as the source of energy will be extremely beneficial. Accordingly, the design of micro-hydro turbine for the resources is essential and significant to establish the national generator of the renewable energy. To winkle the successful time for designing and developing the high-efficient turbine, the reverse engineering was applied to study the characteristics of the flow patterns over the low-head bulb turbine, operating at Pak-mun dam. The Computational Fluid Dynamics (CFD) was exploited as the analytical and investigative tools. The comparison of the fluid mechanical efficiency between CFD simulation and experimentation from the company was well-agreed. In addition to the quantitative comparison, the qualitative patterns of turbine, operating at the maximum efficiency were clarified. Accordingly, the advantage from this study will be exploited for the further design of the low-head bulb turbine and development of the designed-turbine efficiency.

1. Introduction

Since September 6, 2002, the small hydropower research group has been found to study and do research work for developing the small hydro turbine as well as discharge the governmental policy, declaring that within the year of 2011, Thailand has to utilize the renewable energy up to the amount of 8% of entire national energy. Our group was responsible for the water energy to generate the electricity.

Currently, the development of the huge dam is extremely difficult, because of withstanding from various organizations. Therefore, the evaluation of the existent usable water resources for maximum advantage is the main task of our group. The water resource, Mae Ping, was used as the case study to develop the small hydro turbine. The first designed and constructed hydro turbine is the 50 kW bulb turbine [1] and the runner diameter is 0.65 m. The turbine was operated at average water head of 3 m with the approximately 80 % efficiency.

The Pak-mun hydro turbine is also bulb turbine and attains the 92 % efficiency. Developing hydro turbine to achieve the high efficiency and performance needs to accumulate the knowledge and experience more than 20 years. To winkle the time of amassing knowledge for developing hydro turbine, the reverse engineering procedure was applied to attain the highest efficiency within the short period.

This research work was organized as follows. After the conclusion of the mathematical flow governing equations and corresponding models, the model of Pak-mun turbine and numerical simulation were discussed. Investigating the predictive ability of the turbulence models was initially investigated. Consequently, both qualitative and quantitative data were brought together to describe the flow fields and hydrodynamic force generation mechanisms of the turbine. Finally, all of the results would be concluded and hinted to be useful to the people, who concern the hydrodynamics of low-head bulb turbine.

2. Mathematical Models

To describe the turbulent phenomenon, the modification of Navier-Stokes equations (NSEs) was established by Reynolds averaging method, generally used to transform NSEs [2],[3].

By taking time average over the characteristic time of mean values, the instantaneous quantities of direct numerical simulation (DNS) equations were replaced by mean quantities and the additional unknown terms, describing the turbulence, were introduced.

Flow Governing Equations

The modified NSEs, called Reynolds-Averaged Navier-Stokes (RANS) equations, can be written in the tensor form as

$$\frac{\partial \rho}{\partial t}+\frac{\partial(\rho \cdot u_i)}{\partial x_i}=0 \qquad (1)$$

$$\frac{\partial(\rho \cdot u_i)}{\partial t}+\frac{\partial(\rho \cdot u_i \cdot u_j)}{\partial x_j} = -\frac{\partial p}{\partial x_i}+\frac{\partial}{\partial x_j}\left[\mu \cdot \left(\frac{\partial u_i}{\partial u_j}+\frac{\partial u_j}{\partial u_i}-\frac{2}{3}\cdot \delta_{ij}\cdot \frac{\partial u_l}{\partial x_l}\right)\right]+\tau_{ij} \qquad (2)$$

The additional unknown terms were named Reynolds Stress and defined as

$$\tau_{ij}=\frac{\partial\left(\rho \cdot \overline{u_i' \cdot u_j'}\right)}{\partial x_j}$$

Boussinesq Hypothesis

The common fashion, used to model Reynolds Stress term, employs Boussinesq hypothesis, relating the Reynolds Stress with the velocity gradients:

$$\tau_{ij}=\mu_t \cdot \left(\frac{\partial u_i}{\partial x_j}+\frac{\partial u_j}{\partial x_i}\right)-\frac{2}{3}\cdot\left(\rho \cdot k+\mu_t \cdot \frac{\partial u_i}{\partial x_i}\right)\cdot \delta_{ij} \qquad (3)$$

Modeling turbulent eddy viscosity

For the calculation of turbulence flow, the effect of turbulent eddy motions was described and incorporated into the turbulent viscosity term (μ_t). In contrast to the molecular viscosity, the eddy viscosity depends strongly on the flow property. Therefore, selecting the turbulent model, accommodated the flow behavior of each application, is very important.

To attain the accurate prediction of turbine hydrodynamics, the predictive ability of four different turbulent models, including traditional $k-\varepsilon$ turbulent, RNG $k-\varepsilon$, Reynolds Stress, and SST $k-\omega$ turbulent models were investigated. The turbulent models for eddy viscosity were briefly described as follows.

Standard $k-\varepsilon$ Turbulent Model

For the standard $k-\varepsilon$ Model, the turbulent viscosity is computed by the combination of the turbulence kinetic energy k and its dissipative rate ε as follows

$$\mu_t=\rho \cdot C_\mu \cdot \frac{k^2}{\varepsilon} \qquad (4)$$

The k and ε were obtained from the following equations

$$\rho \cdot \frac{Dk}{Dt}=\frac{\partial}{\partial x_i}\cdot\left[\left(\mu+\frac{\mu_t}{\sigma_k}\right)\cdot \frac{\partial k}{\partial x_j}\right]+\mathrm{P}-\rho \cdot \varepsilon \qquad (5)$$

and

$$\rho \cdot \frac{D\varepsilon}{Dt}=\frac{\partial}{\partial x_j}\cdot\left[\left(\mu+\frac{\mu_t}{\sigma_\varepsilon}\right)\cdot \frac{\partial \varepsilon}{\partial x_i}\right]+C_{1\varepsilon}\cdot \frac{\varepsilon}{k}\cdot P-C_{2\varepsilon}\cdot \rho \cdot \frac{\varepsilon^2}{k} \qquad (6)$$

P represents the production of turbulent kinetic energy. The σ_k , σ_ε , $C_{1\varepsilon}$ and $C_{2\varepsilon}$ are constant.

RNG $k-\varepsilon$ Turbulent Model

The RNG-based $k-\varepsilon$ turbulent model is derived from the instantaneous NSEs, using the mathematical technique, renormalized group (RNG) model. The application of RNG theory yields the differential equation for the turbulent viscosity:

$$d\left(\frac{\rho^2 \cdot k}{\sqrt{\varepsilon \cdot \mu}}\right)=1.72\cdot \frac{\mu_{eff}/\mu}{\sqrt{(\mu_{eff}/\mu)-1+C_\upsilon}}\cdot d(\mu_{eff}/\mu) \qquad (7)$$

The equations for the k and ε have the similar form to the standard $k-\varepsilon$ model:

$$\rho \cdot \frac{Dk}{Dt}=\frac{\partial}{\partial x_i}\cdot\left[\alpha_k \cdot \mu_{eff}\cdot \frac{\partial k}{\partial x_j}\right]+\mathrm{P}-\rho \cdot \varepsilon \qquad (8)$$

and

$$\rho \cdot \frac{D\varepsilon}{Dt}=\frac{\partial}{\partial x_j}\cdot\left[\alpha_\varepsilon \cdot \mu_{eff}\cdot \frac{\partial \varepsilon}{\partial x_i}\right]+C_{1\varepsilon}\cdot \frac{\varepsilon}{k}\cdot P-C_{2\varepsilon}\cdot \rho \cdot \frac{\varepsilon^2}{k} \qquad (9)$$

Term P represent the production of turbulent kinetic energy. The quantities α_k and α_ε are inverse effective Prandtl Number of k and ε , respectively, $C_{1\varepsilon}$ and $C_{2\varepsilon}$ are constant.

SST $k-\omega$ Turbulent Model

The eddy viscosity for $k-\omega$ turbulent model is related as follows

$$\mu_t = \rho \cdot \frac{k}{\omega} \cdot \frac{1}{\max\left[\frac{1}{\alpha^*, \frac{\Omega \cdot F_2}{a_1 \cdot \omega}}\right]} \tag{10}$$

The Ω presents mean rate of rotation and F_2 is the blending function. α^* is given by

$$\alpha^* = \alpha^* \cdot \left(\frac{\alpha_0^* + \mathrm{Re}_t / R_k}{1 + \mathrm{Re}_t / R_k} \right) \tag{11}$$

where

$$\mathrm{Re}_t = \frac{\rho \cdot k}{\mu \cdot \omega}, \; R_k = 6, \; \alpha_0^* = \frac{\beta_t}{3} \text{ and } \beta_t = 0.072$$

The equations used to model the complex flow behaviors of the turbulent flow were k and ϖ equations and expressed as follows.

$$\frac{D(\rho \cdot k)}{Dt} = \frac{\partial}{\partial x_j}\left(\Gamma_k \cdot \frac{\partial k}{\partial x_j}\right) + G_k - Y_k + S_k \tag{12}$$

and

$$\frac{D(\rho \cdot \omega)}{Dt} = \frac{\partial}{\partial x_j}\left(\Gamma_\omega \cdot \frac{\partial \omega}{\partial x_j}\right) + G_\omega - Y_\omega + D_\omega + S_\omega \tag{13}$$

G_k and G_ω represent the production of k and ω ,respectively, while Y_k and Y_ω present the dissipation of k and ω. Γ_k and Γ_ω are the effective diffusivity for k and ω

Reynolds Stress Model (RSM)

The Reynolds Stress Model involve in the calculation of individual Reynolds Stress term. The exact transport equation of Reynolds Stress can be written in the following form.

$$\begin{aligned}
&\frac{\partial}{\partial t}\left(\rho \cdot \overline{u_i' \cdot u_j'}\right) + \frac{\partial}{\partial x_k}\left(\rho \cdot u_k \cdot \overline{u_i' \cdot u_j'}\right) = \\
&-\frac{\partial}{\partial x_k}\left[\rho \cdot \overline{u_i' \cdot u_j' \cdot u_k'} + \overline{p\left(\delta_{kj} \cdot u_i' + \delta_{ik} \cdot u_j'\right)}\right] \\
&+\frac{\partial}{\partial x_k}\left[\mu \frac{\partial}{\partial x_k}\left(\overline{u_i' \cdot u_j'}\right)\right] \\
&-\rho \cdot \left(\overline{u_i' \cdot u_k'} \cdot \frac{\partial u_j}{\partial x_k} + \overline{u_j' \cdot u_k'} \cdot \frac{\partial u_i}{\partial x_k}\right) + p \cdot \left(\frac{\partial u_i'}{\partial x_j} + \frac{\partial u_j'}{\partial x_i}\right) \\
&-2 \cdot \mu \cdot \overline{\frac{\partial u_i'}{\partial x_k} \cdot \frac{\partial u_j'}{\partial x_k}} - 2 \cdot \rho \cdot \Omega_k \cdot \left(\overline{u_j' \cdot u_m'} \cdot \varepsilon_{ikm} + \overline{u_i' \cdot u_m'} \cdot \varepsilon_{jkm}\right)
\end{aligned} \tag{14}$$

The fist and second terms of left hand side of the equations is the local time derivative and convection, C_{ij} , respectively. The fist term of right hand side of the RSM equations represents turbulent diffusion, $D_{T,ij}$ and followed by the terms of molecular diffusion, $D_{L,ij}$ and stress production, P_{ij} .The forth terms present the pressure strain, ϕ_{ij} .Finally, the last two terms are Dissipation, ε_{ij} and the production by system rotation F_{ij} ,respectively.

The terms of C_{ij} , $D_{L,ij}$, P_{ij} , and F_{ij} do not require any modeling. Nevertheless, $D_{T,ij}$, ϕ_{ij} , and ε_{ij} need to be modeled.

3. Turbine Configurations and CFD Methods

The commercial CFD code, Fluent, was used to predict the turbine efficiency of the Pak-mun configurations. The model is composed of the hub, shroud, inlet guide vane (IGV), and the turbine blade, presented via Figure 1.

The time-independent incompressible Navier-Stokes equations and the various turbulent models were discretized using the finite volume method. QUICK and central differencing

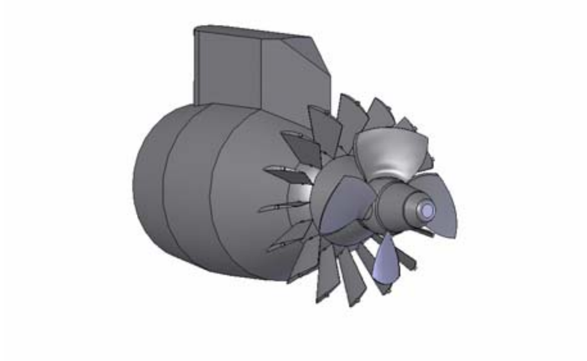

(a)

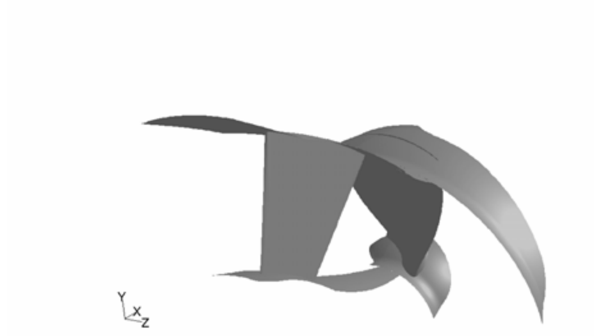

(b)

Figure 1. The geometries of (a) the actual turbine and (b) the computational turbine

flow numerical schemes were applied for convective and diffusive terms, respectively. The discrete nonlinear equations were implemented implicitly. To evaluate the pressure field, the pressure-velocity coupling algorithm SIMPLE (Semi Implicit Method for Pressure-Linked Equations) was selected. The linearized equations were solved using multigrid method. Due to the geometrical complexity of the turbine and guide vane, the numerically approximated equations were performed on the collocated tetrahedral grid. The grids of IGV and turbine regime were constructed separately, comprising approximate total of 960,000 cells, shown in figure 2. Generating mesh at the interface between the domain of the IGV and turbine blade, is nonconformal.

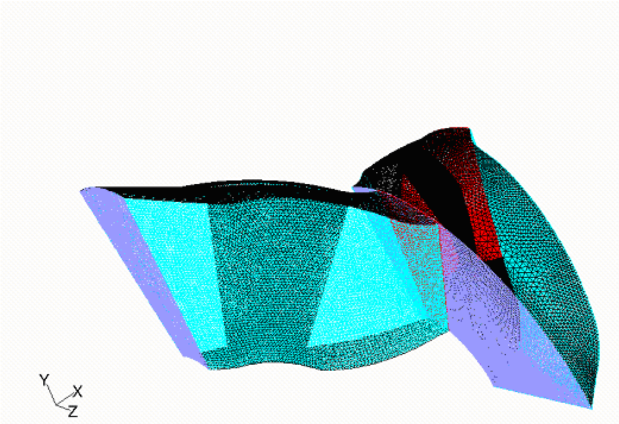

Figure 2. The grid distribution of the computational domain

4. Simulation Description and Boundary Condition Imposition

The flow equations and the turbulent models were performed on the computational domains in figure 2. To reduce the computational effort, the single blade of the actual model was utilized for the simulation. The guide vane blade is stationary, while the runner was operated at the constant rotational speed. The inflow boundary was imposed by uniform and constant velocity, whereas the outlet constant pressure was applied at the flow departure. The lateral boundaries were periodic. For the hub, shroud, guide vane, and turbine blade, the non-slip boundary condition was specified. At the interface boundary between the IGV and runner regions, the flow and turbulent properties are circumferentially averaged on both IGV outlet and runner inlet. The averaged data are then used to update the boundary conditions of two zones.

5. Results and Discussions

In the discussions of presented investigation, the validation on the CFD models was first discussed and then, followed by describing hydrodynamics of the highest efficiency of the low-head bulb turbine.

CFD Validation

To assess the predictive ability of various turbulent models, the maximum turbine efficiency from simulation and experimentation are compared as indicated in the table 1. The maximum turbine efficiency is obtained from the ratio of the delivered work to the turbine blade to the available energy from the fluid stream.

Table1. The comparison of the hydraulic efficiency between various turbulence models and the experimentation [4]

Model	$k-\varepsilon$	RNG $k-\varepsilon$	SST $k-\omega$	RSM	Experiment
Hydraulic%	90.54	94.56	93.70	94.74	91.00

Of the hydraulic efficiency from the various turbulence models, the computational results are close and in the good agreement with the result from the experimentation. The maximum deviation is about 4 % by using RSM. Surprisingly, despite no improvement for the swirl and curvature flow domination, the excellent agreement was provided by the standard $k-\varepsilon$ model.

Flow Pattern Analysis

According to the earlier turbulent model validation, the standard $k-\varepsilon$ model was chosen to investigate the flow field over the turbine.

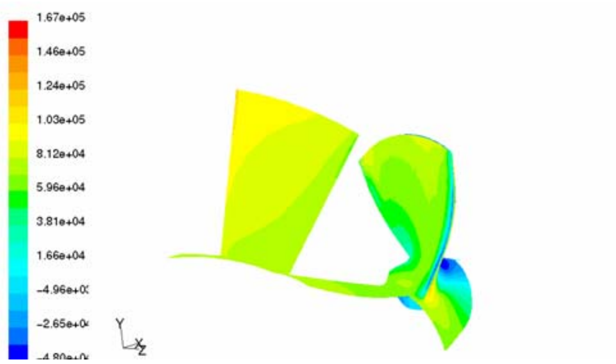

Figure 3. The pressure distribution for the IGV and runner

As shown in figure 3, the pressure distribution of IGV varies along the height of IGV and streamwise direction because of the deflection of flow orientation from linear momentum to angular momentum to establish the appropriate angle of the flow before attacking the turbine blades. The divergence configuration of the bulb resulted in the radial variation of the fluid momentum as exhibited in the figure 4 (a) and (b). As a result, the non-uniform flow pattern was produced before entering the runner, whereas the radially and axially uniformly-distributed pressure pattern at the vicinity of the flow departure behide the turbine blade was observed.

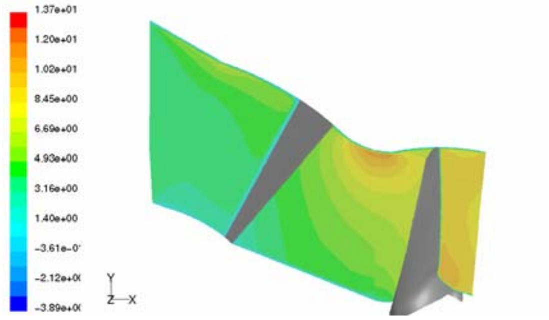

(a) Axial velocity Distribution

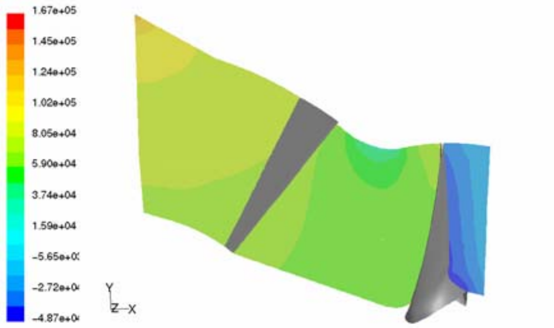

(b) Pressure Distribution

Figure 4. The contour plot of (a) velocity and (b) pressure

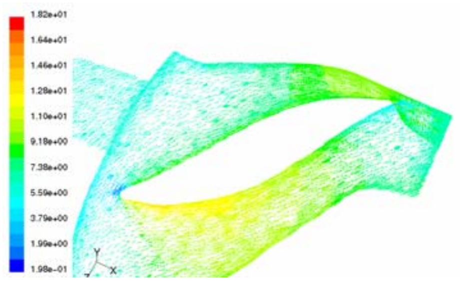

(a) Runner root

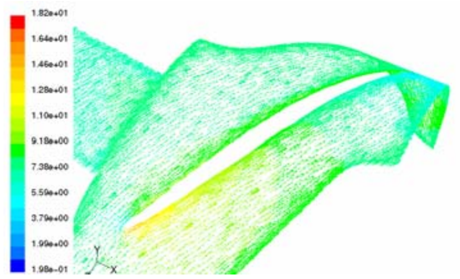

(b) Runner middle

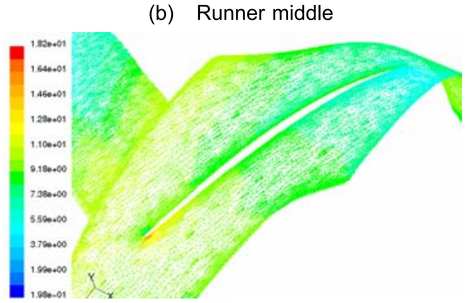

(c) Runner tip

Figure 5. The velocity vector at (a) root, (b) middle, and (c) tip

As clearly seen from picture 5, the runner thickness becomes larger and larger from hub to tip. The circumferentially uniform flow patterns were established before approaching the runner domain, consistent with the theory of the computation at the interface zone. As expected, there is no flow separation on the runner.

Figure 6 shows the plot of pressure coefficients (Cp) at the base, middle, and tip positions along the runner blade.

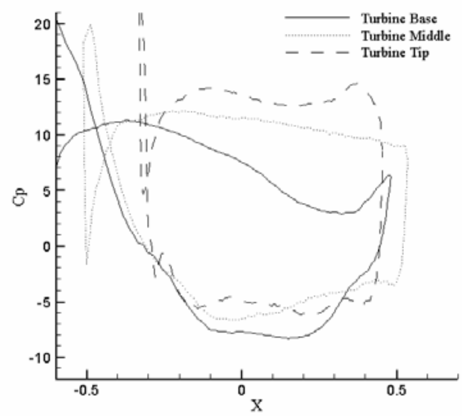

Figure 6. The plot of pressure coefficients along the turbine blade

It was found that the more slender of the blade, the stronger discontinuity of pressure distribution around the leading and trailing edge. The pressure coefficients at all positions are distributed uniformly both suction and pressure sides, leading to the uniform pressure drop along the runner and the pressure gradient between suction and pressure sides is not much different.

6 Conclusion and Recommendation

The procedure of Computational Fluid Dynamics was exploited to establish the knowledge and insight into the flow behavior of the low-head bulb turbine. Four turbulence models, including traditional $k-\varepsilon$ turbulent, RNG $k-\varepsilon$, Reynolds Stress, and SST $k-\omega$ turbulent models were brought to investigate the predictive ability of the low-head bulb turbine simulation. The flow governing equations and the relevant models with QUICK numerical scheme were implemented on the tetrahedrons.

In the calculation of the hydraulic efficiency, all of turbulence models yield the good harmony with the experimental result. The best agreement was accomplished by standard $k-\varepsilon$ model. This is because of that there have no the off stream line from the turbine surface. By reverse engineering, the excellent turbine efficiency can be achieved by avoiding the flow separation and uniformly delivering the energy of intermediate working fluid to the entire turbine blade.

The further research will be focused on the capitation effect on the turbine blades using multiphase model.

7. References

[1] Tiaple Y. and Nontakaew U., The development of bulb turbine for low head storage using CFD simulation, The joint international conference on "Sustainable Energy and Enviroment (SEE)", 2004.

[2] Anderson, J. D., et al. (1992) Introduction to computational fluid dynamics, Edited by Wendt, John F, New York : Spriger-Verlag.

[3] Chung, T. J. (2002) Computational fluid dynamics, Cambridge : Cambridge University press.

[4] Abfalterer, J., Report on model test for Pak-mun Hydroelectric project, 1991.